Transactions of the Korean Nuclear Society Autumn Meeting
Gyeongju, Korea, October 24-25, 2013

Effect of Residual Strain Induced by Cold Working on PWSCC of Alloy 690

Sung-Woo Kim*, Seong-Sik Hwang, Yun-Soo Lim
Nuclear Materials Division, Korea Atomic Energy Research Institute, Daejeon 305-353, Korea
**Corresponding author: kimsw@kaeri.re.kr*

1. Introduction

Nickel-based alloys such as Alloy 600 and 690 have been used as structural materials in a pressurized water reactor (PWR) because of their high corrosion resistance. However, many forms of corrosion have been reported in specific conditions of materials and environments [1]. The most severe corrosion is stress corrosion cracking (SCC) of nickel-based alloys, which is called PWSCC for primary water stress corrosion cracking in the primary cooling water, and ODSCC for outside diameter stress corrosion cracking in the secondary cooling water. PWSCC has been widely reported to occur in the inside of the steam generator (SG) tubing [2], and in other instrumentation nozzles such as the control rod drive mechanism (CRDM) penetrations [3], especially on those surfaces having a dissimilar metal welds (DMW) or those heavily machined.

Under an abnormal working procedure or without a sufficient post-heat treatment for stress relaxation, a high tensile stress can persist after welding or cold working of the alloys. Variation of a strain field is also accompanied by the cold working or machining process. The conventional method for measuring the residual strain is a micro-hardness test, which has a limitation owing to the presence of precipitates and grain boundaries in the matrix of the test specimen. A new technique of electron backscatter diffraction (EBSD) has recently been applied to residual strain analysis on a micro-scale to overcome this limitation [4]. This work is concerning a quantitative analysis of the local residual strain by EBSD and its effect on the PWSCC of Alloy 690 CRDM materials.

2. Experimental

The cold worked specimens of Alloy 690 were prepared by a one-dimensional rolling process with different strain levels of 0, 10, 20, 30 and 40% at room temperature. The Vickers hardness was measured using a conventional micro-hardness test. EBSD measurements were carried out on the etched surface of the cold worked specimens with an image resolution of 256 pixels × 256 pixels. To characterize the local strain at the micro-scale, a Kernel average misorientation (KAM) and a grain-average misorientation (GAM) were introduced as appropriate parameters for the quantification of the local strain. KAM is defined for a given spot or pixel as the numerical average misorientation of that spot in comparison to its nearest neighbors, and GAM is calculated as the average value of KAM within the grain.

The crack growth rate (CGR) of the cold worked specimens was measured by a direct-current potential drop (DCPD) method [5] in a primary water chemistry simulated for typical PWR operating conditions, i.e., in a solution of 1,200 ppm B as H_3BO_3, and 2.2 ppm Li as LiOH, at 340 and 360 ^oC. The dissolved oxygen (DO) content and dissolved hydrogen (DH) content in the solution became steady below 5 ppb and at 2.7 ppm, respectively. The inlet conductivity and pH of the solution were about 23 μS/cm and 6.4, respectively. The solution was continuously circulated using a water loop system with a high-pressure diaphragm pump, and the water chemistry was monitored using in-line sensors.

3. Results and discussion

Fig. 1 presents inverse pole figure (IPF) images derived using an EBSD analysis for the Alloy 690 cold-worked specimens at various strain levels, indicating the orientations of each grain on the specimen surface with different colors. As compared to the specimen that was solution-annealed (0% strain level) showing one principal orientation per grain (Fig. 1(a)), the highly strained specimen revealed significant alteration of the orientation within the grains owing to a local deformation (Fig. 1(b), (c) and (d)).

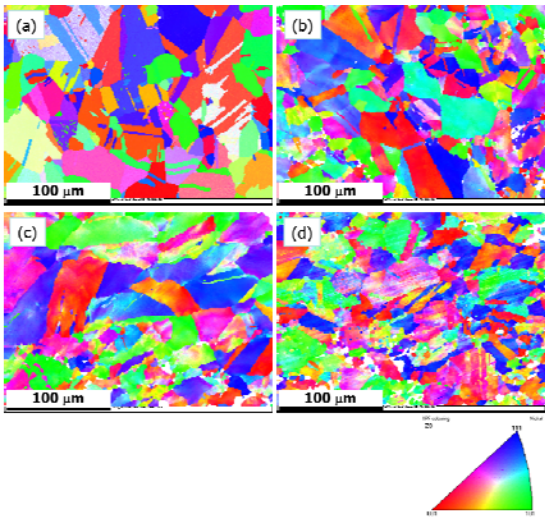

Fig. 1. IPF images of Alloy 690 cold-rolled at plastic strain levels of (a) 0%, (b) 10%, (c) 20%, and (d) 30% measured using an EBSD with a step size of 1 μm.

Fig. 2 shows KAM maps obtained from the EBSD results of Alloy 690 cold-worked specimen at various

strain levels. It is clearly shown that the KAM value increased with the plastic strain level, while that value is nearly zero for Alloy 690 when solution-annealed (Fig. 2(a)); this trend is more remarkable at the grain boundary of the cold-rolled specimen (Fig. 2(b), (c) and (d)).

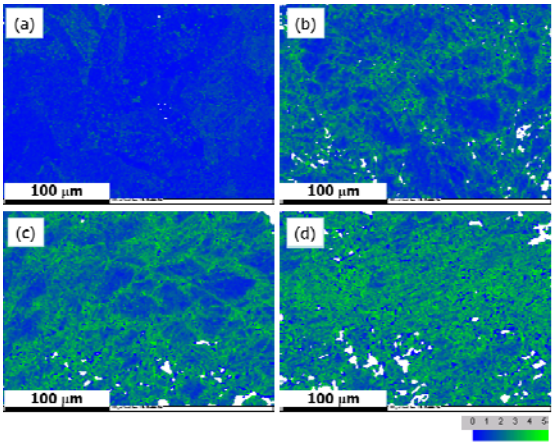

Fig. 2. KAM maps of Alloy 690 cold-rolled at plastic strain levels of (a) 0%, (b) 10%, (c) 20%, and (d) 30% calculated from EBSD results.

The GAM value was also obtained from the EBSD results for a comparison with the Vickers hardness measured by the conventional method to validate the strain analysis by EBSD, as shown in Fig. 3. The relationship between the GAM value and the strain level showed a good agreement with the dependence of the hardness value on the strain level, indicating that a strain analysis by EBSD is a promising technique applicable to quantify the local strain formed in nickel-based alloys, especially at the micro-scale without any interference by the grain boundary or precipitates.

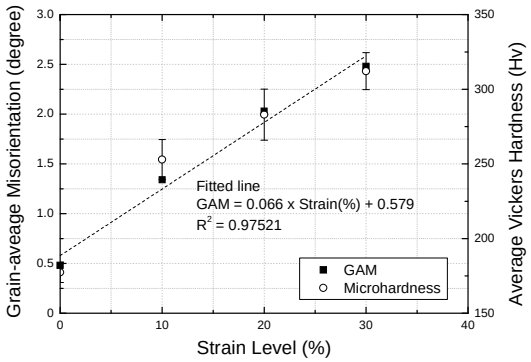

Fig. 3. Plots of GAM values vs. strain level measured by EBSD analysis, and average Vickers hardness obtained by a microhardness measurement for Alloy 690 cold-rolled at various plastic strain levels.

Fig. 4 demonstrates the dependence of CGR on the stress intensity factor (K) applied to Alloy 690 cold-worked at plastic strain levels of 0 and 40%, measured at 340 and 360 °C. With an increase in the K value and solution temperature, the CGR of all specimens increased. Furthermore, the heavily cold-worked specimen showed higher CGR by 10 times as compared to the specimen solution-annealed (0% strain level), and more interestingly, close to MRP-55 curve of Alloy 600. It is clear that the residual strain concentrated at the grain boundary accelerated the crack growth along the boundary. After the CGR test, a microstructural analysis of the cracked surface will be performed to verify the CGR measured by DCPD and to explain the effect of residual strain induced by cold-working on the PWSCC CGR of Alloy 690 CRDM materials.

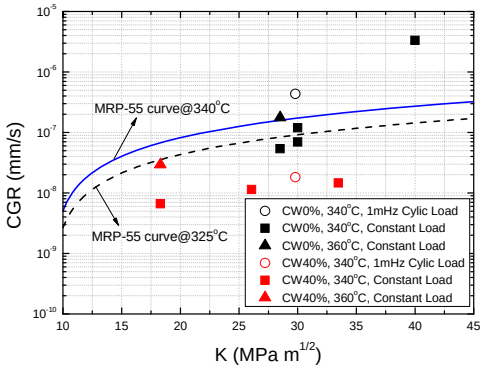

Fig. 4. Dependence of CGR on K applied to Alloy 690 specimens cold-worked at plastic strain levels of 0 and 40%, measured at 340 and 360 °C.

4. Conclusions

In this work, the local residual strain of Alloy 690 CRDM materials cold-worked at various plastic strain levels was quantitatively evaluated using an EBSD analysis. From KAM maps, it was confirmed that the residual strain increased with cold-working, and a higher strain was concentrated at the grain boundary than in the matrix. The severe strain field localized at the grain boundary accelerated the inter-grannular growth of PWSCC of Alloy 690.

REFERENCES

[1] D. Feron and J. M. Olive (eds), Corrosion Issues in Light Water Reactors - Stress Corrosion Cracking, European Federation of Corrosion Publishing, New York, 2013.
[2] J. M. Sarver, EPRI Workshop on Intergranular Corrosion and Primary Water Stress Corrosion Cracking Mechanisms. EPRI, Palo Alto, p. C11/1, 1987.
[3] H. Xu, S. Fyfitch, J. W. Hyres, 12th International Conference on Environmental Degradation of Materials in Nuclear Power System – Water Reactors, TMS, Salt Lake City, p 833, 2005.
[4] Z. Lu, T. Shoji, S. Yamazaki, K. Ogawa, Corros. Sci., Vol. 58, p. 211, 2012.
[5] ASTM Standard Test Method for Measurement of Fatigue Crack Growth Rates, ASTM International, West Conshohocken, E 645-05, 2005.